

Metal Organic Frameworks Synthesis: The Versatility of Triethylamine

Wei Zhang^{*[a, b]} and Nicola Pinna^{*[a]}

Metal Organic Frameworks (MOFs) are organic-inorganic hybrid materials with exceptionally customizable composition and properties. MOFs intrinsically possess open metal sites, tunable pore size/shape and an ultra-large specific surface area, and have obtained significant attention over the past 30 years. Furthermore, through the integration of functional moieties such as, molecules, functional groups, noble metal clusters and nanocrystals or nanoparticles into MOFs, the resulting composites have greatly enriched the physical and chemical properties

of pure MOFs, enabling their application in a wider range of fields. Triethylamine (TEA) as an organic base has consistently played a fundamental role in the development of MOFs. In this Concept, the versatility of triethylamine when involved in the synthesis of MOFs is discussed. Four sections are used to elaborate on the role of TEA including: (1) Single crystal synthesis; (2) Size and morphology control; (3) Counterion of MOFs; (4) MOFs composites synthesis. In the last part, we highlight the potential of TEA for further developments.

1. Introduction

Metal-organic frameworks (MOFs), also known as porous coordination polymers (PCPs), are crystalline organic-inorganic hybrid materials, formed by periodical complexation of metal nodes and organic ligands.^[1] To date, thousands of MOFs have been reported and increasing attention has been devoted to the field. The intrinsically highly adjustable topological structures and customized chemical properties endow MOFs with a very high surface area, a large number of open metal sites, and a three-dimensional periodic pore/channel system.^[2] These tunable properties make MOFs an ideal platform with significant prospects for applications in catalysis, biomedicine, gas storage and separation, energy storage and electronic devices.^[3]

The introduction of novel approaches to control the synthesis of MOFs for specific needs has always been at the center of focus. First of all, the synthesis of MOF single crystals is required to obtain its crystal structure by single crystal x-ray diffractometry. Therefore, synthesizing high-quality single crystals is almost a prerequisite to solve complicated topological structures. Secondly, controlling the size and morphology is required because the properties of MOFs can be strongly influenced by many factors such as morphology, including

exposed facets and particle size.^[4] Thirdly, the design of new topological structures by choosing different building blocks has been highly pursued to enrich the MOFs library. Lastly, the incorporation of functional moieties such as molecules, noble metal clusters, and nanocrystals into MOFs has been considered as a useful strategy to obtain multifunctional composite materials.^[5] Therefore, exploiting suitable synthesis strategies to meet specific demands has always been a highly active research topic in the MOFs community.

For the majority of MOFs, their crystal growth process typically involves two steps. First, the deprotonation of the organic ligands. Followed by the coordination of the deprotonated ligands to the metal ions, forming a periodical framework. In most of the cases, the deprotonation process is the rate-determining step and has exhibited significant influence on the nucleation and growth of MOFs. To date, various solvents, excess of organic ligands (beyond the stoichiometric ratio), addition of a base, and other parameters, including temperature and pressure, have been used to control the deprotonation process.^[6] Amongst the deprotonation agents used including diethylamine, n-hexamine, NaOH and ammonium hydroxide,^[7] triethylamine (TEA) as a mild and volatile organic base, is widely applied in the synthesis of MOFs, facilitating the formation of single-crystal MOFs and enabling control over shape/morphology, or size.^[8] Furthermore, we recently made use of TEA to successfully synthesize diverse single-crystal MOF nanohybrids, amorphous MOFs and coatings, further enriching the applicability of TEA as deprotonating agent in MOFs.^[9]

Although TEA is widely utilized in MOF synthesis, to date, there is no relevant literature comprehensively summarizing its application. In this concept article, we will summarize the crucial role of TEA in the development of MOFs.

[a] Dr. W. Zhang, Prof. N. Pinna
 Department of Chemistry and The Center for the Science of Materials Berlin
 Humboldt-Universität zu Berlin
 Brook-Taylor-Strasse 2, 12489 Berlin (Germany)
 E-mail: zhangweq@hu-berlin.de
 nicola.pinna@hu-berlin.de

[b] Dr. W. Zhang
 Department of Colloid Chemistry
 Max Planck Institute of Colloids and Interfaces
 Am Mühlenberg 1, 14476 Potsdam, Germany

© 2024 The Authors. Chemistry - A European Journal published by Wiley-VCH GmbH. This is an open access article under the terms of the Creative Commons Attribution Non-Commercial NoDerivs License, which permits use and distribution in any medium, provided the original work is properly cited, the use is non-commercial and no modifications or adaptations are made.

2. Synthesis of Single-Crystal MOFs

Triethylamine is a common organic base and used in many organic synthesis.^[10] In the early stages of MOFs research, TEA played a crucial role in synthesizing new single-crystal MOFs as well.^[6a,11] In 1997, using TEA vapor as a deprotonating agent was firstly introduced to synthesize MOFs, and a new single-crystal MOFs ($\text{Zn}_2\text{BTC}(\text{NO}_3)$) with a 3-D porous network was successfully obtained (Figure 1).^[6a] In a typical synthesis, TEA vapor was generated in a large vial and allowed to gradually diffuse into a small vial containing MOFs precursors (zinc nitrate and 1,3,5-benzenetricarboxylic acid (H_3BTC)). The TEA promotes the deprotonation of the H_3BTC ligands. Compared to the previously used pyridine ($\text{pK}_a=5.21$), the stronger base TEA ($\text{pK}_a=11.01$) allows for the complete deprotonation of the H_3BTC ligands into BTC^{3-} ions. In addition, the metal ions also exhibit poor binding affinity for TEA compared to pyridine. Therefore, the fully “activated” BTC^{3-} ligands can coordinate to the zinc ions to form the 3-D porous structure. Slowly introducing TEA through vapor diffusion can be used to effectively control the deprotonation rate of H_3BTC , thereby regulating the nucleation and growth of the MOFs. The successful synthesis of large single crystals through the TEA diffusion method allowed for an easier determination of the crystal structure. The TEA vapor diffusion method has been later applied to the synthesis of many new MOFs single crystals.^[11] This significantly enriched the MOFs library in the early stages.

3. Size and Morphology Control

3.1. Size control

In many applications, MOFs display significant morphology or size-dependent properties.^[4,12] For example, a size-induced molecular-scale shape-memory effect has been firstly found in a flexible porous coordination polymer (PCP) of $[\text{Cu}_2(\text{dicarboxylate})_2(\text{amine})]_n$.^[12a] Normally, this crystal structure exhibits a flexible and reversible deformation during the adsorption/desorption of the guest molecules. However, when downsizing these micrometer-sized crystals to meso-sized crystals, their framework undergoes a dramatic transition from reversible flexibility to shape-memory behavior. For meso-sized

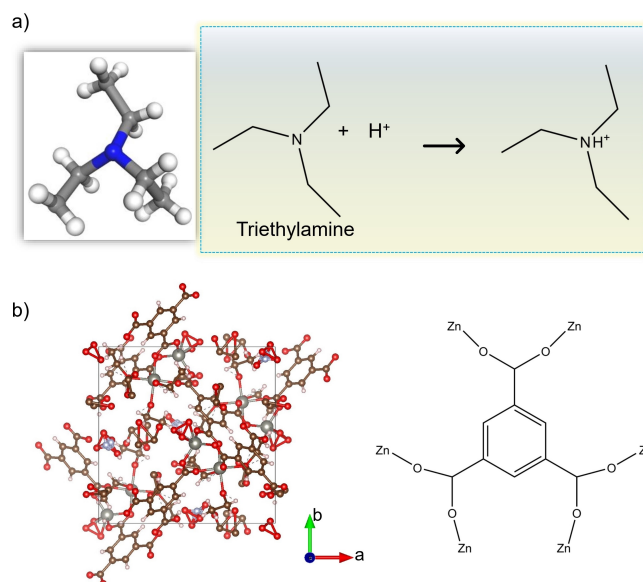
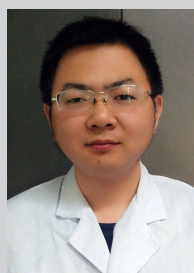


Figure 1. (a) The utilization of triethylamine as a deprotonation agent. (b) A schematic representation of $\text{Zn}_2\text{BTC}(\text{NO}_3)$.

crystals, a temporary open phase can be maintained after desorption of guest molecules, and recovers the original phase under further thermal treatment. These results indicate that crystal size could be used to control structural mobility through surface energy regulation induced by crystal downsizing. Furthermore, crystal downsizing has also been demonstrated as a strategy to enhance the storage capacity of guest molecules.^[12b] The coordination framework crystals ($\text{Fe}(\text{py})_2[\text{Pt}(\text{CN})_4]_n$) of 135 nm show no significant capability for guest uptake. However, when downsizing crystals to nanometer-sized thin-film forms, they exhibit obvious dynamic guest adsorption isotherms. Besides, other size-dependent gas sorption and magnetic property have also been investigated in previous reports.^[12c,d] Therefore, size modulation is important for the tuning of MOFs properties.

In classical crystallization theory, the initial nucleation rate and subsequent growth rate determine the final size of the resulting product. TEA exhibited the capability to deprotonate organic ligands in synthesis of single-crystal MOFs. TEA can also be used to tune the MOFs size by regulating the nucleation and



Wei Zhang received his Ph.D. in condensed physics at East China Normal University (ECNU) in 2018. Afterward, he continued with three years of postdoctoral research at ECNU. In 2021, he started to work at the Department of Chemistry at the Humboldt University of Berlin as a research fellow. His research area involves synthesis of various nanostructures of coordination polymers for energy conversion and storage applications.



Nicola Pinna received his Ph.D. in physical chemistry from the Université Pierre et Marie Curie in 2001. He has since worked at the Fritz Haber Institute of the Max Planck Society, the Max Planck Institute of Colloids and Interfaces, the Martin Luther University of Halle-Wittenberg, the University of Aveiro, and the Seoul National University. In July 2012 he joined the Department of Chemistry of the Humboldt University of Berlin as professor of inorganic chemistry. His research activity focuses on the development of novel materials chemistry routes to nanostructured materials for energy and environmental applications.

growth rate. For example, Lu *et al.* reported the synthesis of monodisperse octahedral UiO-66 ($Zr_6O_4(OH)_4(BDC)_6$, BDC = deprotonated terephthalic acid) crystals with varying sizes by simply adjusting the amount of TEA.^[13] In Figure 2, when the concentration of TEA gradually increases from 0.5 mM to 1, 2, 4, 6, and 8 mM, the corresponding average particle size decreases from 2140 to 1134, 742, 554, 529, and 512 nm, respectively. The results clearly indicate a significant correlation between the crystal size and the initial amount of added TEA. The greater the amount of triethylamine added, the smaller the particle size. In this synthesis, H_2BDC needs to undergo deprotonation first, becoming activated as BDC^{2-} ion, and then the BDC^{2-} ion can coordinate to the Zr nodes to form the UiO-66 crystals. Here, TEA has the ability to regulate the nucleation rate via the deprotonation process of H_2BDC into BDC^{2-} . Lower is the amount of triethylamine added, the slower is the initial nucleation rate, and the fewer the crystal nuclei are, thereby favoring the formation of larger-sized crystals. To date, TEA has been successfully used to control the crystal size in numerous MOFs systems such as ZIF-67, MOF-5, HKUST-1, MOF-74.^[8b,14]

3.2. Morphology control

Morphology is also a crucial factor influencing the properties of MOFs.^[15] Shape-dependent exposed facets usually exhibit different properties, especially in catalysis. For instance, a cubic crystalline MOF (NENU-3a) with only {100} facets with more active sites display significantly enhanced catalytic activities in biodiesel production compared to an octahedron covered by {111} facets.^[15a] Morphology control has also been extended to regulate other MOFs, and considered as effective strategy to regulate their properties.^[15b] In addition to the size, TEA has also

been demonstrated to play a fundamental role in controlling the morphology of MOFs, especially in 2D MOFs.^[8a,16] Ge *et al.* reported the successful synthesis of 2D MOF-Fe/Co by using TEA as a modulator agent. Without the addition of TEA, the slow deprotonation process of H_2BDC results in bulk MOFs (Figure 3).^[8a] Introducing some amounts of TEA into the reaction solution facilitates the deprotonation of 1,4-BDC carboxylic acids, accelerates their coordination with metal ions, and simultaneously produces a small amount of OH^- ions in water, effectively stabilizing the edges of 2D MOF layers (Figure 3). The OH^- ions generated from TEA and water are crucial for the stabilization of 2D MOFs and ultimately lead to the formation of MOF-Fe/Co nanosheets. The nanosheets, with an enhanced active surface area, display excellent electrocatalytic activity and exhibit superior OER performance when compared to bulk MOFs. Besides, TEA has been demonstrated to be effective in the synthesis of 2D MOFs in other studies.^[16]

4. Counterions of MOFs

In addition to its deprotonation capability, TEA can also serve as a counterion for synthesizing new MOFs topological structures. For example, in the structure of $[Cd_3(BTC)_3(H_2O)] \cdot (HTEA) \cdot 2(H_2O)$,^[17] the protonated form of TEA ($HTEA^+$) was used as a counterion into the Cd-BTC framework, providing electroneutrality to the entire crystal. In Figure 4, the crystal structure exhibits two distinct channels of different sizes. The $HTEA^+$, serving as the guest molecule ion, is situated within the smaller channel and is connected to the framework through hydrogen bonds. Kim *et al.* successfully synthesized various Zn-based MOFs using HTEA as a counterion. These include $Zn(ADC)_2 \cdot (HTEA)_2$ (MOF-31; ADC = acetylenedicarboxylate),

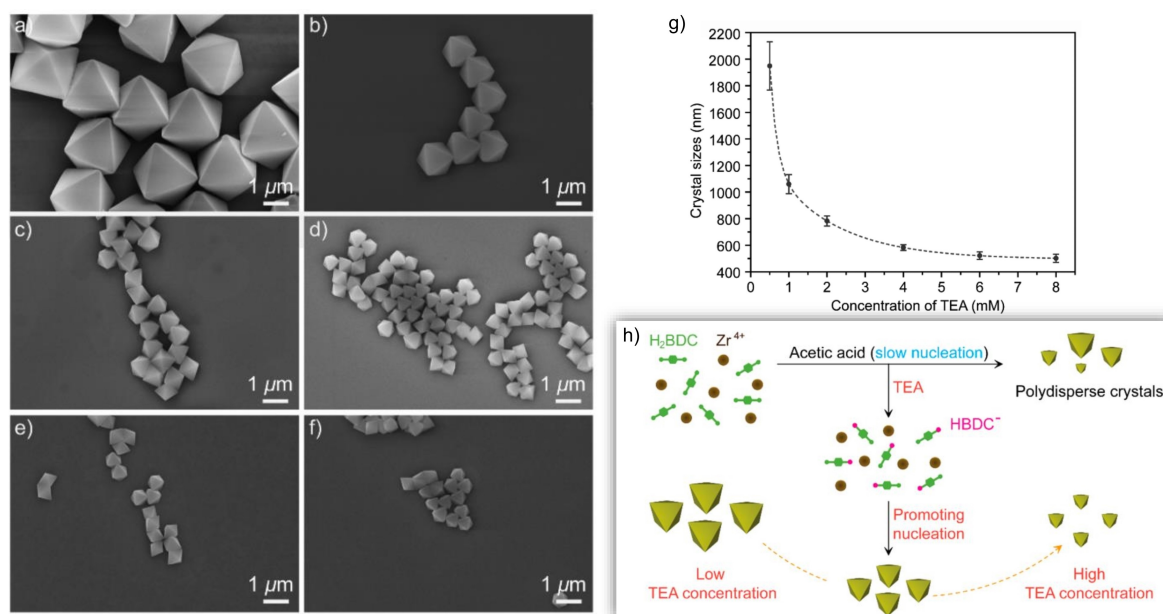


Figure 2. (a–f) SEM images of UiO-66 in the presence of TEA with varying concentrations ranging from 0.5 mM to 1, 2, 4, 6, and 8 mM, respectively. (g) Statistical average particle sizes of UiO-66 versus TEA concentrations. (h) A schematic illustration of the synthesis process of UiO-66 modulated by TEA. Reproduced with permission.^[13] Copyright © 2017 American Chemical Society

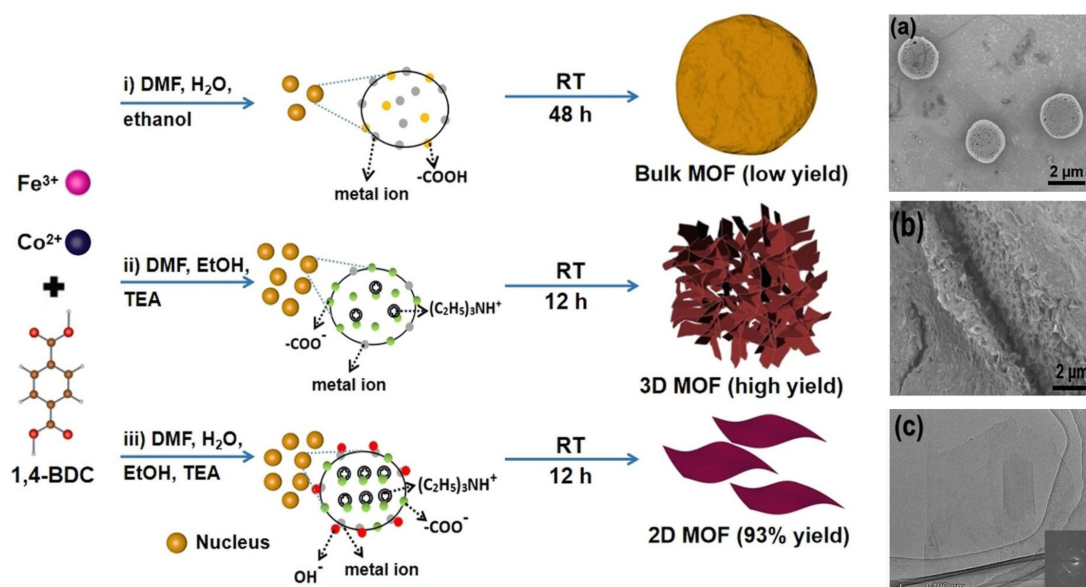


Figure 3. A schematic illustration of the synthesis of bulk, 3D, and 2D MOFs. (a) SEM image of bulk MOFs obtained in mixture solution of DMF, H₂O and ethanol without TEA. (b) SEM image of 3D MOFs obtained in mixture solution of DMF and ethanol with a certain amount of TEA. (c) SEM image of 2D MOFs nanosheet obtained in mixture solution of DMF, H₂O and ethanol with a certain amount of TEA. Reproduced with permission.^[8a] Copyright 2021, Wiley-VCH.

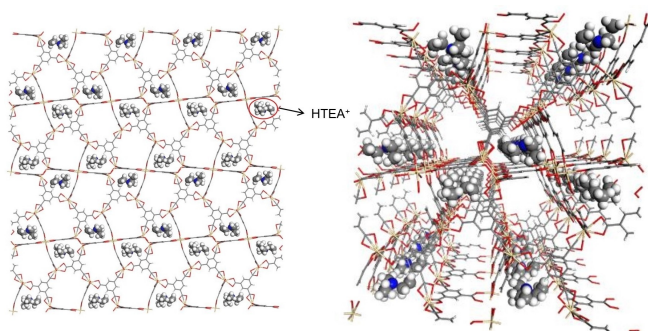


Figure 4. Crystal structure of HTEA⁺ molecules in [Cd₃(BTC)₃(H₂O)] · (HTEA) · 2(H₂O).

Zn₂(NDC)₃ · [(HTEA)(DEF)(ClBz)]₂ (MOF-37; NDC = 2,6-naphthalenedicarboxylate), and Zn₃O(BTC)₂ · (HTEA)₂ (MOF-38; BTC = benzenetricarboxylate).^[18] In addition, three new Co-based MOFs have been reported by incorporated HTEA⁺ as a counterion to stabilize the structure.^[19] To date, protonated TEA has been widely used in the synthesis of MOFs.^[20]

5. Synthesis of MOF Composites

5.1. Integration of MOFs onto a substrate

Growth of MOFs onto diverse substrates to form films or membranes and into varying templates to form composites has attracted significant attention due to their applications in electronic device and energy storage and conversion.^[21]

The liquid surface has been considered as an ideal platform for the confined synthesis of films, due to its molecular flatness and absence of defects.^[22] By coupling the TEA diffusion

method with confinement at the air-liquid interface, smooth and compact MOF films could be obtained. For instance, Yuan *et al.* proposed a simple strategy to fabricate centimeter-sized Ni₃(HITP)₂ (HITP = 2,3,6,7,10,11-hexaminothriphenylene) films by using the TEA diffusion method.^[22d] MOFs precursors including NiCl₂ and 2,3,6,7,10,11-hexaminothriphenylene-6HCl (HATP) were first dissolved in deionized water to form clear solution. Then, pure TEA in a small vial was sealed with another vial containing the MOF precursors in a beaker without stirring. TEA vapor is generated and then gradually diffuses toward the reaction solution, entering at the air-liquid interface. The TEA triggered the deprotonation process of HATP and the confined formation of Ni₃(HITP)₂ at air-liquid interface (Figure 5). Finally, uniform and compacted MOFs films can be formed at the confined interface and transferred onto other substrates for the fabrication of electronic devices.

In addition, by introducing 3D porous templates at the air-liquid interface, single-crystal MOFs could be formed at the inner void of porous template to generate MOFs composites.^[23] Briefly, a centimeter-sized porous template assembled from conductive carbon black particles is placed in the MOFs precursor solution near the air-liquid surface.^[23b] Subsequently, the reaction solution containing porous template and pure TEA liquid were sealed within a beaker, and the reaction system was kept in an aged state without stirring. Similar to the previous process, TEA vapor promotes the deprotonation of ligands within the porous template, facilitating the subsequent nucleation and growth of the MOFs. MOF crystals gradually grow inside the template, eventually filling the voids of the porous template to form MOF composites. The TEA diffusion method was also used to incorporation of MOF nanoparticles into hypercrosslinked styrene-maleic acid (SMA) copolymer beads to successfully fabricate MOFs-SMA bead composite.^[23a]

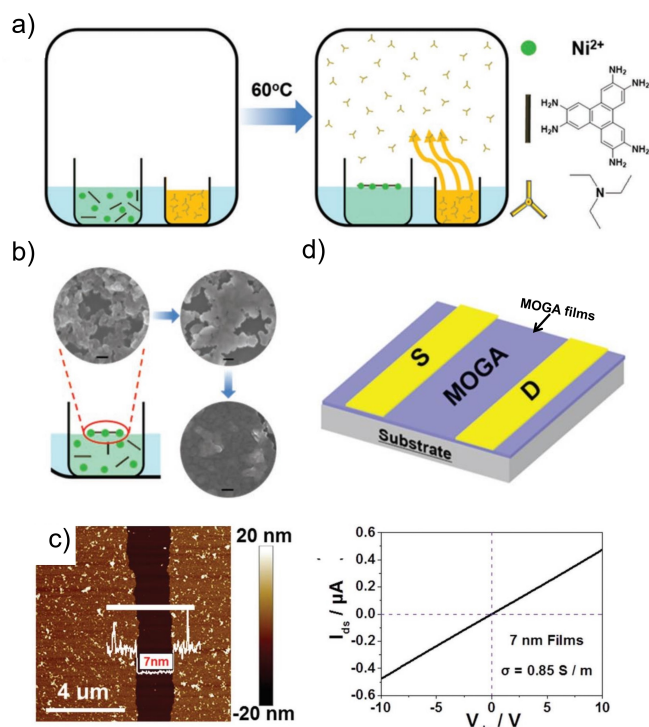


Figure 5. (a) Illustration of synthesis of MOGA ($\text{Ni}_3(\text{HITP})_2$) films using TEA vapor diffusion method. (b) The formation process of MOGA films. (c) Topographic AFM and AFM height images of 7 nm films and the corresponding I-V curves of device. (d) The schematic illustration of MOGA film-based device. Reproduced with permission.^[22d] Copyright 2019, Wiley-VCH.

5.2. Integration of NPs into MOFs

Contrary to process of integrating MOFs onto substrates or into templates, incorporation of diverse functional NPs into single-crystal MOFs to generate multifunctional MOFs nanohybrids has also been widely investigated in many applications such as catalysis, sensing and filtration. However, a universally applicable synthesis method for MOF-nanohybrids, covering the full diversity of all conceivable core-shell combinations, has always posed a challenge.

Recently, our group has proposed a universal simple strategy to synthesis diverse MOF nanohybrids by using the TEA diffusion method.^[9a] In this work, slow diffusion rate of TEA vapor is the key of this synthesis process. Figure 6 illustrates the schematic diagram of a synthesis set up. One vial contains the MOF precursors, core-NPs, and solvent, sealed with a cap with one hole (1 mm in diameter). Another vial contains pure TEA in ethanol with a ratio of 1:3, closed by a cap with three holes. These two vials were sealed in a 500 mL beaker. Throughout the reaction, the mother solution is stirred gently. Compared to the previous TEA vapor diffusion method, this set up presents some distinct differences. Firstly, the ethanolic solution of triethylamine is used as a substitute to pure TEA. This allows to more effectively reduce and control the diffusion rate of TEA vapor. Secondly, compared to the previous open system, sealing with a cap including a small hole can further reduce the diffusion rate of TEA vapor. Lastly, maintaining gentle stirring

can overcome the inhomogeneity caused by the TEA vapor diffusion across the gas-liquid interface.

ZIF-67 was used as a typical MOFs in this case to illustrate the synthesis approach. Similar to the previous synthesis, TEA promotes the deprotonation step of the organic ligand of 2-methylimidazole. The gradual diffusion of TEA induces the slow release of 'activated' deprotonated 2-methylimidazole ions, thereby triggering heterogeneous nucleation of ZIF-67 on core-NPs (β -FeOOH nanorods). Throughout the slow growth process, a significant quantity of β -FeOOH nanorods was encapsulated within ZIF-67, ultimately resulting in the formation of single-crystal multi- β -FeOOH@ZIF-67 nanohybrids. Moreover, by modulating the initial core concentration, we can easily obtain multi- β -FeOOH@ZIF-67 nanohybrids with core contents ranging from 5% to 40%. When we used NO_3^- ions to replace competing Cl^- anions coordinating the metal ions, a singular β -FeOOH@ZIF-67 was obtained. The heterogeneous nucleation induced by the slow diffusion of TEA vapor enables this method to be independent of the shape and the properties of the core nanoparticles. In our work, six core-NPs including Ag, Au, NaYF_4 , $\text{Ni}_3[\text{Fe}(\text{CN})_6]_2$, Fe_2O_3 and β -FeOOH were selected and successfully incorporated into single-crystal ZIF-67. The same deprotonation process strategy of organic ligands can be applied in the formation of many MOFs. Therefore, we successfully extended the approach to ZIF-67 nanohybrids synthesis to other types of MOFs including ZIF-8, ZIF-zn, NJU-30, HKUST-1, MIL-88(Fe), and MOF-74(Co), demonstrating the generality of this strategy.

For this synthesis, the diffusion rate of TEA vapor shows a significant impact on nucleation of MOFs, thus influencing their morphology and size. A slower diffusion rate could induce a slower crystallization nucleation rate, thereby resulting in the formation of larger-sized crystals. Moreover, the slow crystallization nucleation and growth process guides the MOF growth toward an equilibrium shape, ultimately yielding single-crystal MOFs with a Wulff shape. The fundamental prerequisite for this successful synthesis is that the organic ligand possesses acidic sites, which must undergo a deprotonation process during the formation of the MOF. The slow diffusion of TEA induces a gradual deprotonation process of the ligand, resulting in a preferential heterogeneous nucleation on the surface of functional nanoparticles. As a result, the basicity of the counter anion will influence the deprotonation process of the ligand, thereby exhibiting a significant impact on this synthesis. Therefore, in this work, nitrate ions or chloride ions are chosen as anions with weaker basicity to synthesize various MOFs by using TEA vapor diffusion method. On the contrary, the anions with relatively high basicity such as acetate ions could accelerate the deprotonation process of the ligand. This, in turn, affects TEA's control over the deprotonation process, leading to the ineffectiveness of the method. In previous reports, many MOF systems exhibit extreme stability under specific condition. For instance, ZIF-67 displays superior thermal stability at temperatures even higher than 300 °C,^[24a] and HKUST-1 demonstrates impressive humidity stability.^[24b] Here, the slow TEA vapor diffusion method guarantees the synthesis of single-crystal MOFs including ZIF-67 or HKUST-1. The perfect single-crystal form will be more beneficial to ensure intrinsic chemical

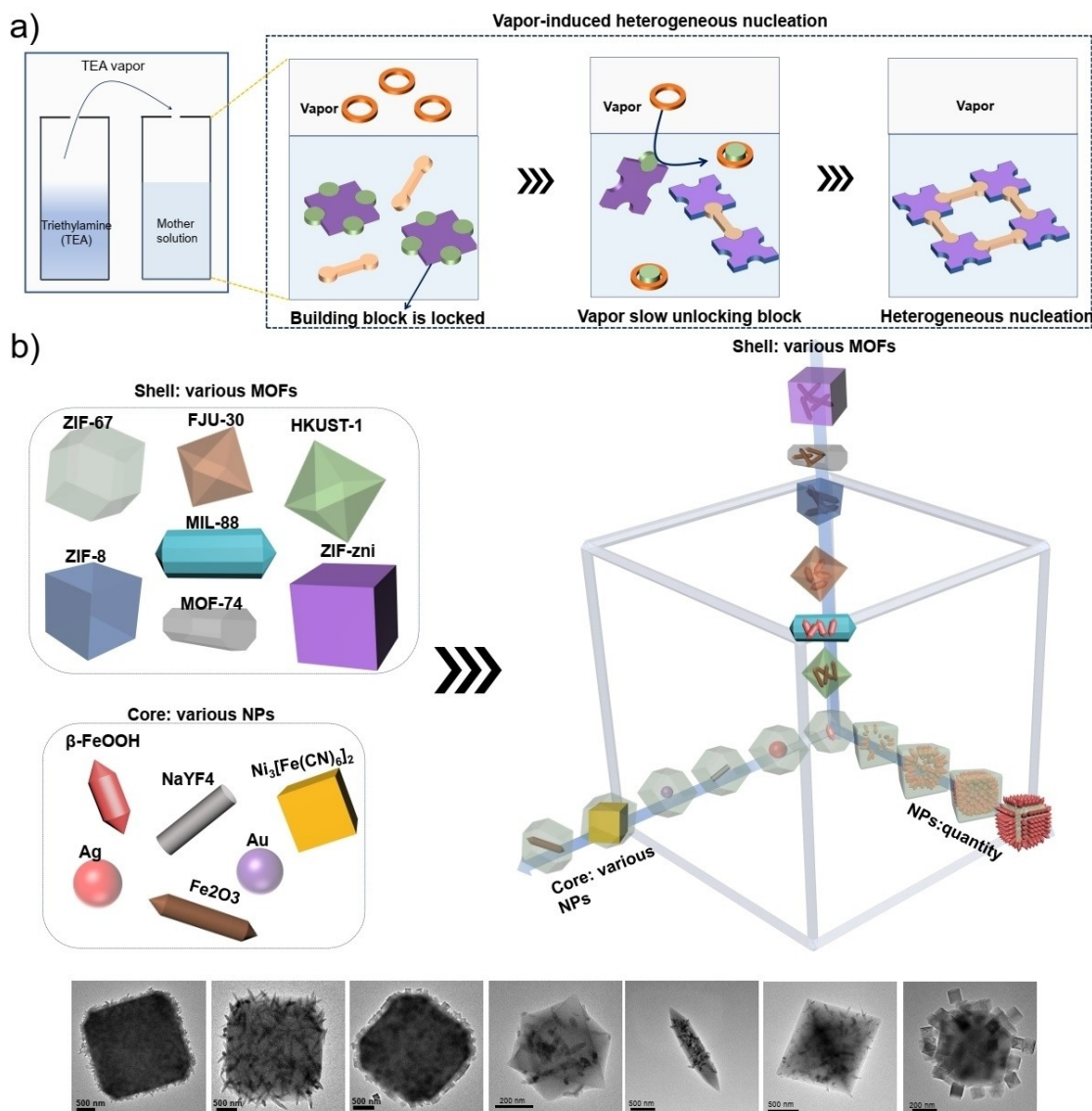


Figure 6. (a) A schematic illustration of the TEA vapor diffusion method for synthesizing various MOF nanohybrids. (b) The 3D models of various types of MOFs, NPs and the MOF nanohybrids, and some selected TEM images of MOF nanohybrids. Reproduced with permission.^[9a] Copyright 2023, Wiley-VCH.

stability. For example, the obtained single-crystal ZIF-67 exhibited excellent structural stability after storage for two months or thermal treatment at 300 °C.

Additionally, our group also used TEA to synthesize more complex composite structures. Noble metal nanocrystals were successfully integrated into hollow ZIF-67 cubic shell via a self-sacrificial template method under the assistance of TEA (Figure 7a).^[9b] Hollow structure was formed by the dissolution of the interior part of ZIF-67 seed and re-growth onto the shell. The TEA facilitates the growth of the shell by accelerating the deprotonation process of 2-methylimidazole. During this process, PVP-stabilized noble metal nanocrystals are encapsulated within the newly formed shell, ultimately resulting in the formation of hollow composites.

5.3. Amorphous MOFs colloids and coatings

Recently, we reported a simple method to synthesize various amorphous MOFs colloids by mimicking the Stöber method.^[9c] Similar to amorphous SiO₂ synthesis, there are many MOFs whose crystallization process is mainly influenced by kinetics. By applying the TEA diffusion method into these types of MOFs, monodisperse amorphous MOFs spheres and conformal coatings were successfully obtained by a controllable sol-gel-like process (Figure 7b–c).^[9c] Like the ammonia in the Stöber method, TEA used here can act as a base to regulate the sol-gel process. The slow diffusion of TEA vapor ensures the gradual release of deprotonated organic ligands, and then controls the kinetics of complexation between deprotonated ligands and metal nodes. By introducing pre-formed nanoparticles into the reaction solution, uniform amorphous MOFs shell can be deposited on seeds to form conformal core-shell colloids. The

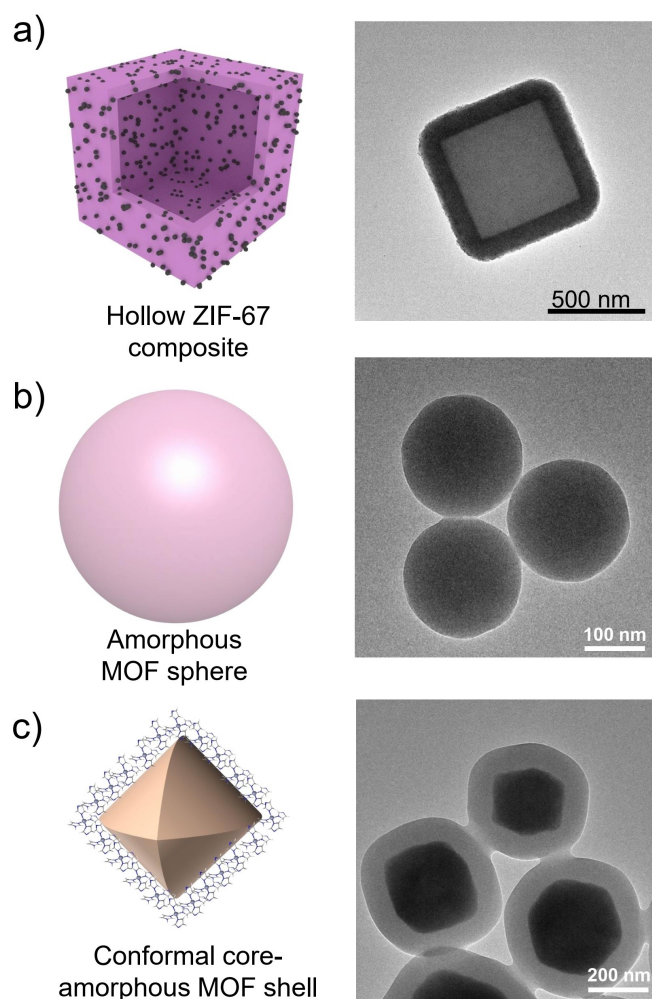


Figure 7. (a) 3D model and TEM image of Pd@hollow ZIF-67 composite. (b) 3D model and TEM image of amorphous MOF sphere. (c) 3D model and TEM image of conformal core-amorphous MOFs shell. Reproduced with permission.^[9b] Copyright © 2023 American Chemical Society

conformal coating process is independent of the substrate properties and can be extended to the fabrication of diverse core-shell structures.

6. Summary and Outlook

This concept article highlights the versatility of triethylamine in the synthesis of MOFs. It can be divided into four aspects. 1) In order to characterize the crystal structure of new MOFs, TEA was used to synthesize high-quality MOF single crystals. 2) TEA can be used to modulate the size and morphology of MOFs. 3) As a part of the MOFs, the protonated TEA molecule is incorporated into the channel to obtain novel neutral MOFs crystals. 4) Through the utilization of the TEA diffusion method, amorphous MOFs colloids, MOF composites such as MOF films and coatings, and MOF nanohybrids can be obtained.

Although the TEA vapor diffusion strategy has been successfully used in several MOFs, there are still some limitations. First, this method is not applicable to organic

ligands that are not deprotonated during this process. In addition, the TEA vapor is hazardous. The emission of TEA generated from industry including a catalyst in polymerization reactions and an intermediate as a corrosion inhibitor in the manufacturing of diverse chemicals has attracted considerable attention.^[25] For large-scale synthesis, collected and recycled TEA vapor should be taken into consideration. To date, a bio-filter has been investigated and shows superior performance in removal of TEA vapor from air.^[25] In this case, recycling could be achieved by introducing N_2 as carrier gas to push the excess of TEA vapors into ethanol to form a solution. The resulting ethanolic TEA solution can be used as a TEA vapor generator in MOF synthesis.

Based on the precise control of the diffusion of TEA vapor, our group has developed a universal strategy for synthesizing MOF nanohybrids. This also opens up new possibilities for the application of TEA in MOFs. Firstly, the properties of obtained MOF and MOF composites, such as functional stability and storage stability, need further investigation for specific applications. Furthermore, to meet the requirements of various applications, the slow TEA diffusion method could be extended to synthesize additional multifunctional MOF nanohybrids by selecting different types of MOF and core-NPs. Additionally, this slow diffusion method shows promise for being extended to the synthesis of high-crystallinity MOF thin films on different substrates. Lastly, the controlled synthesis of amorphous MOFs has always been a significant challenge. The TEA diffusion method provides a simple and general synthesis pathway. This provides a solid foundation for future research on the properties of amorphous MOFs. We believe that the slow TEA diffusion method to the synthesis of MOFs can play an important role in various fields in the future.

Acknowledgements

W.Z. thanks the Alexander von Humboldt Foundation, Bonn, Germany, for a postdoctoral fellowship and research grant. This work was partially financed by the Max Planck Society. Open Access funding enabled and organized by Projekt DEAL.

Conflict of Interests

The authors declare no conflict of interest.

Data Availability Statement

Data sharing is not applicable to this article as no new data were created or analyzed in this study.

Keywords: Metal Organic Frameworks · Composite · Triethylamine · Deprotonation · Morphology

- [1] a) O. Yaghi, H. Li, T. Groy, *J. Am. Chem. Soc.* **1996**, *118*, 9096–9101; b) S. Kitagawa, R. Kitaura, S. i. Noro, *Angew. Chem. Int. Ed.* **2004**, *43*, 2334–2375; c) W. Zhang, L. Xia, C. Shi, R. Qi, M. Hu, *Matter* **2023**, *6*, 3394–3412.
- [2] H. Furukawa, K. E. Cordova, M. O’Keeffe, O. M. Yaghi, *Science* **2013**, *341*, 1230444.
- [3] a) F. Vermoortele, B. Bueken, G. Le Bars, B. Van de Voorde, M. Vandichel, K. Houthoofd, A. Vimont, M. Daturi, M. Waroquier, V. Van Speybroeck, *J. Am. Chem. Soc.* **2013**, *135*, 11465–11468; b) Q. Wang, D. Astruc, *Chem. Rev.* **2019**, *120*, 1438–1511; c) P. Horcajada, R. Gref, T. Baati, P. K. Allan, G. Maurin, P. Couvreur, G. Férey, R. E. Morris, C. Serre, *Chem. Rev.* **2012**, *112*, 1232–1268; d) R.-B. Lin, S. Xiang, W. Zhou, B. Chen, *Chem* **2020**, *6*, 337–363; e) W. Zhang, W. Chen, X. Zhao, Q. Dang, Y. Li, T. Shen, F. Wu, L. Tang, H. Jiang, M. Hu, *Angew. Chem. Int. Ed.* **2019**, *58*, 7431–7434; f) Y. Li, Q. Dang, C. Shi, W. Zhang, C. Jing, X. Li, M. Hu, *J. Mater. Chem. A* **2019**, *7*, 23084–23090.
- [4] K. Suresh, D. Aulakh, J. Purewal, D. J. Siegel, M. Veenstra, A. J. Matzger, *J. Am. Chem. Soc.* **2021**, *143*, 10727–10734.
- [5] a) S. Dai, A. Tissot, C. Serre, *Adv. Energy Mater.* **2022**, *12*, 2100061; b) Y. Yun, H. Sheng, K. Bao, L. Xu, Y. Zhang, D. Astruc, M. Zhu, *J. Am. Chem. Soc.* **2020**, *142*, 4126–4130.
- [6] a) O. Yaghi, C. E. Davis, G. Li, H. Li, *J. Am. Chem. Soc.* **1997**, *119*, 2861–2868; b) L. Feng, K.-Y. Wang, J. Powell, H.-C. Zhou, *Matter* **2019**, *1*, 801–824.
- [7] a) H. Bunzen, M. Grzywa, M. Hambach, S. Spirkel, D. Volkmer, *Cryst. Growth Des.* **2016**, *16*, 3190–3197; b) M. He, J. Yao, Q. Liu, Z. Zhong, H. Wang, *Dalton Trans.* **2013**, *42*, 16608–16613.
- [8] a) K. Ge, S. Sun, Y. Zhao, K. Yang, S. Wang, Z. Zhang, J. Cao, Y. Yang, Y. Zhang, M. Pan, *Angew. Chem. Int. Ed.* **2021**, *60*, 12097–12102; b) W. Zhang, X. Jiang, X. Wang, Y. V. Kaneti, Y. Chen, J. Liu, J. S. Jiang, Y. Yamauchi, M. Hu, *Angew. Chem. Int. Ed.* **2017**, *129*, 8555–8560.
- [9] a) W. Zhang, M. J. Bojdys, N. Pinna, *Angew. Chem. Int. Ed.* **2023**, *62*, e202301021; b) W. Zhang, N. Pinna, *Chem. Mater.* **2023**, *35*, 6799–6807; c) W. Zhang, Y. Liu, H. Jeppesen, N. Pinna, *ChemRxiv*. **2023**, DOI: 10.26434/chemrxiv-2023-m7g7w.
- [10] H. C. Brown, E. Negishi, J. J. Katz, *J. Am. Chem. Soc.* **1972**, *94*, 5893–5894.
- [11] a) H. Li, M. Eddaoudi, M. O’Keeffe, O. M. Yaghi, *Nature* **1999**, *402*, 276–279; b) R. N. Devi, M. Edgar, J. Gonzalez, A. M. Slawin, D. P. Tunstall, P. Grewal, P. A. Cox, P. A. Wright, *J. Phys. Chem. B* **2004**, *108*, 535–543.
- [12] a) Y. Sakata, S. Furukawa, M. Kondo, K. Hirai, N. Horike, Y. Takashima, H. Uehara, N. Louvain, M. Meilikhov, T. Tsuruoka, S. Isoda, W. Kosaka, O. Sakata, S. Kitagawa, *Science* **2013**, *339*, 193–196; b) S. Sakaida, K. Otsubo, O. Sakata, C. Song, A. Fujiwara, M. Takata, H. Kitagawa, *Nat. Chem.* **2016**, *8*, 377–383; c) D. Tanaka, A. Henke, K. Albrecht, M. Moeller, K. Nakagawa, S. Kitagawa, J. Groll, *Nat. Chem.* **2010**, *2*, 410–416; d) H. Peng, S. Tricard, G. Félix, G. Molnár, W. Nicolazzi, L. Salmon, A. Bousseksou, *Angew. Chem. Int. Ed.* **2014**, *126*, 11074–11078.
- [13] Y. Zhao, Q. Zhang, Y. Li, R. Zhang, G. Lu, *ACS Appl. Mater. Interfaces* **2017**, *9*, 15079–15085.
- [14] a) S. Wang, Y. Lv, Y. Yao, H. Yu, G. Lu, *Inorg. Chem. Commun.* **2018**, *93*, 56–60; b) F. Wang, H. Guo, Y. Chai, Y. Li, C. Liu, *Microporous Mesoporous Mater.* **2013**, *173*, 181–188; c) J. Hu, Y. Chen, H. Zhang, Z. Chen, Y. Ling, Y. Yang, X. Liu, Y. Jia, Y. Zhou, *Microporous Mesoporous Mater.* **2021**, *315*, 110900.
- [15] a) Y. Liu, S. Liu, D. He, N. Li, Y. Ji, Z. Zheng, F. Luo, S. Liu, Z. Shi, C. Hu, *J. Am. Chem. Soc.* **2015**, *137*, 12697–12703; b) H. J. Lee, W. Cho, S. Jung, M. Oh, *Adv. Mater.* **2009**, *21*, 674–677.
- [16] a) S. Zhao, Y. Wang, J. Dong, C.-T. He, H. Yin, P. An, K. Zhao, X. Zhang, C. Gao, L. Zhang, *Nat. Energy* **2016**, *1*, 1–10; b) A. K. Chaudhari, H. J. Kim, I. Han, J. C. Tan, *Adv. Mater.* **2017**, *29*, 1701463.
- [17] Q. Fang, G. Zhu, M. Xue, Z. Wang, J. Sun, S. Qiu, *Cryst. Growth Des.* **2008**, *8*, 319–329.
- [18] J. Kim, B. Chen, T. M. Reineke, H. Li, M. Eddaoudi, D. B. Moler, M. O’Keeffe, O. M. Yaghi, *J. Am. Chem. Soc.* **2001**, *123*, 8239–8247.
- [19] H.-S. Lu, L. Bai, W.-W. Xiong, P. Li, J. Ding, G. Zhang, T. Wu, Y. Zhao, J.-M. Lee, Y. Yang, *Inorg. Chem.* **2014**, *53*, 8529–8537.
- [20] a) X. Yu, Y. S. Toh, J. Zhao, L. Nie, K. Ye, Y. Wang, D. Li, Q. Zhang, *J. Solid State Chem.* **2015**, *232*, 14–18; b) S. Qiu, G. Zhu, *Coord. Chem. Rev.* **2009**, *253*, 2891–2911.
- [21] Q. Qian, P. A. Asinger, M. J. Lee, G. Han, K. Mizrahi Rodriguez, S. Lin, F. M. Benedetti, A. X. Wu, W. S. Chi, Z. P. Smith, *Chem. Rev.* **2020**, *120*, 8161–8266.
- [22] a) G. Wu, J. Huang, Y. Zang, J. He, G. Xu, *J. Am. Chem. Soc.* **2017**, *139*, 1360–1363; b) Y. Shen, B. Shan, H. Cai, Y. Qin, A. Agarwal, D. B. Trivedi, B. Chen, L. Liu, H. Zhuang, B. Mu, *Adv. Mater.* **2018**, *30*, 1802497; c) H. Lu, S. Zhu, *Eur. J. Inorg. Chem.* **2013**, *2013*, 1294–1300; d) K. Yuan, T. Song, X. Zhu, B. Li, B. Han, L. Zheng, J. Li, X. Zhang, W. Hu, *Small* **2019**, *15*, e1804845.
- [23] a) R. R. Gonte, P. C. Deb, K. Balasubramanian, *J. Polym.* **2013**, *2013*, 1–8; b) W. Zhang, Y. Li, C. Shi, R. Qi, M. Hu, *J. Am. Chem. Soc.* **2021**, *143*, 6447–6459.
- [24] a) K. S. Park, Z. Ni, A. P. Côté, J. Y. Choi, R. Huang, F. J. Uribe-Romo, H. K. Chae, M. O’Keeffe, O. M. Yaghi, *Proc. Natl. Acad. Sci. USA* **2006**, *103*, 10186–10191; b) J. R. Álvarez, E. Sánchez-González, E. Pérez, E. Schneider-Revueltas, A. Martínez, A. Tejeda-Cruz, A. Islas-Jácome, E. González-Zamora, I. A. Ibarra, *Dalton Trans.* **2017**, *46*, 9192–9200.
- [25] a) B. Gandu, K. Sandhya, A. G. Rao, Y. Swamy, *Bioresour. Technol.* **2013**, *139*, 155–160; b) M. Mirmohammadi, S. Sotoudeheian, R. Bayat, *Int. J. Environ. Sci. Technol.* **2017**, *14*, 1615–1624.

Manuscript received: December 20, 2023

Accepted manuscript online: February 1, 2024

Version of record online: March 6, 2024